Available online at www.sciencedirect.com
ScienceDirect
Solid State Ionics 177 (2006) 2227 – 2233
SOLID STATE IONICS
www.elsevier.com/locate/ssi

Transport properties and phase stability of mixed conducting oxide membranes

C.Y. Park [a], D.X. Huang [a], A.J. Jacobson [a,*], L. Hu [b], C.A. Mims [b]

[a] Department of Chemistry, University of Houston, Houston, TX 77204, USA
[b] Department of Chemical Engineering, University of Toronto, Toronto, ON, Canada M5S 3E5

Received 29 January 2006; received in revised form 22 February 2006; accepted 27 February 2006

Abstract

At high strontium doping levels, perovskite oxides containing iron have suitable stability and transport properties for use as oxide ion transport membranes. In our studies of these materials, we have investigated the pO_2 and temperature dependence of the conductivity and non-stoichiometry of $La_{1-x}Sr_xFe_{1-y}M_yO_{3-\delta}$ (M = Cr, Ti) by using electrochemical cells and the thermal expansion by dilatometry. Non-equilibrium behavior is observed in both the chemical expansion data and also in the conductivity and stoichiometry and suggests the occurrence of microscopic phase segregation on reduction. Analysis of the microstructure of quenched samples confirms the occurrence of local phase separation. Bulk diffusion and surface exchange coefficients under near-gradientless conditions have been determined by the electrical conductivity relaxation (ECR) technique and by isotope exchange depth profiling (IEDP). Evaluation of transport under a chemical gradient was accomplished by transient isotopic tracing of operating membranes. The isotope transients ($^{16}O_2$–$^{18}O_2$) were performed on tubular membranes operating at steady state at temperatures between 1023 K and 1173 K and allow an unambiguous separation of surface and bulk resistances to oxygen permeation under steady state conditions, a separation not possible by permeation measurements alone.

Keywords: Ion transport membranes; Surface exchange; Oxygen diffusion; Phase stability

1. Introduction

Mixed ionic electronic conductors (MIECs) with the ABO_3 perovskite or related structures have been widely studied because of their practical applications in ion-transport membranes, pressure-driven oxygen generators, partial oxidation reactors, and as electrodes for solid oxide fuel cells (SOFCs) [1]. A number of materials problems remain outstanding for the application of ion transport membrane reactors in the high oxygen partial pressure gradients found, for example, in *syngas* generation by partial oxidation of methane. The membrane composition must simultaneously provide the necessary oxygen flux and have stability and appropriate mechanical properties over a wide pO_2 range.

The $La_{1-x}Sr_xFeO_{3-x}$ (LSFO) series has high mixed conductivity and better stability than the $La_{1-x}Sr_xCoO_{3-x}$ (LSCO) series but still exhibits limited stability in low-pO_2 environments. Additional substitution on the B-site by metal ions that are more difficult to reduce solves some of these problems but issues remain concerning both kinetic and thermodynamic stability and the effects of composition changes that result from partial decomposition or surface segregation on the membrane surface catalytic properties.

In our studies of membrane materials, we have investigated the pO_2 and temperature dependence of the conductivity, non-stoichiometry and thermal-expansion behavior of two specific compositions, $La_{0.2}Sr_{0.8}Fe_{0.8}Cr_{0.2}O_{3-\delta}$ and $La_{0.2}Sr_{0.8}Fe_{0.55}Ti_{0.45}O_{3-\delta}$, by using electrochemical cells and dilatometry [2–5]. Additional measurements on the simpler composition, $La_{0.5}Sr_{0.5}FeO_{3-\delta}$, have been made for comparison [6]. These and other recent studies of ferrites with the perovskite structure show anomalous behavior at low oxygen partial pressures ($<10^{-5}$ atm). The anomalies are due to non-equilibrium effects and can be avoided by using very strict criteria for the attainment of equilibrium. The slowness of the oxygen

---

* Corresponding author.
E-mail address: ajjacob@uh.edu (A.J. Jacobson).

0167-2738/$ - see front matter © 2006 Elsevier B.V. All rights reserved.
doi:10.1016/j.ssi.2006.02.042

equilibration kinetics and the observation that deviations between equilibrium and non-equilibrium behavior become larger with increasing temperature suggest that cation rearrangements or phase separation must take place. The microscopic details of the mechanism responsible for the slow kinetics are not yet fully understood. In this paper, we present evidence that the slow kinetics are associated with nanoscopic phase separation and suggest a general model that provides a basis for further experiments.

The large chemical gradients in operating oxygen transport membranes bring all of the structural issues above into play. Since variations in the structure and transport properties at any location in the membrane can have a large influence on the entire membrane, it is thus important to evaluate the membrane transport properties under an operating gradient. We have accomplished this by applying a transient isotopic tracing technique to an operating membrane. The evolution of the isotopic transient through the membrane following a pulse of $^{18}O_2$ to the "air" side reveals the surface exchange parameters, their degree of reversibility, and the bulk transport properties in the presence of a large chemical gradient. These results reveal very different values from those obtained under gradientless conditions, suggesting that some of the complex features of the material crystal structure play an important role in the membrane performance.

2. Experiments

Powders of $La_{0.2}Sr_{0.8}Fe_{0.55}Ti_{0.45}O_{3-\delta}$ and $La_{0.2}Sr_{0.8}Fe_{0.8}Cr_{0.2}O_{3-\delta}$, synthesized by using the spray pyrolysis method, were obtained from Praxair Specialty Ceramics (Woodinville, WA). The $La_{0.5}Sr_{0.5}FeO_{3-\delta}$ sample was synthesized by a self-propagating high temperature synthesis (SHS) method [6]. Electrical conductivity measurements were made in sealed electrochemical cells as a function of pO_2 at temperatures from 750 °C to 1000 °C down to 10^{-18} atm for the lowest temperatures. The measurements were made using an AC 4-point technique at a single frequency (1 kHz) and the phase angle monitored to confirm the absence of any polarization effects. Stoichiometry measurements were made in similar sealed electrochemical cells. The details of the sample characterization, conductivity and stoichiometry were reported previously [2–4]. Rectangular sample bars of $La_{0.2}Sr_{0.8}Fe_{0.55}Ti_{0.45}O_{3-\delta}$ sintered at 1450 °C were used for dilatometry measurements (NETZSCH, DIL 402C) [5]. The chemical expansion data were obtained by switching the gas from air to pure argon or by using mixed gases (5% H_2/N_2, CO_2, and argon) in the temperature range between 800 and 1000 °C. The oxygen partial pressure (pO_2) was measured with an oxygen analyzer (AMETEK, TM-1B) at the outlet of the dilatometer.

For microstructural studies, $La_{0.2}Sr_{0.8}Fe_{0.55}Ti_{0.45}O_{3-\delta}$ discs were quenched in air from 900 °C and different partial oxygen pressures ($pO_2 = \sim 1.3\times10^{-4}$, 1.1×10^{-7}, 1.2×10^{-10}, 6.7×10^{-14} atm). For comparison, $La_{0.5}Sr_{0.5}FeO_{3-\delta}$ discs were reduced at 950 °C for 24–48 h in 5% H_2/N_2. Structural studies of quenched and reduced samples were performed by X-ray powder diffraction measurements with CuKα radiation. Powder diffraction patterns of the samples were obtained in 0.01° steps with a preset count time of 5 s, over the range $10° \leq 2\theta \leq 100°$. The $La_{0.2}Sr_{0.8}Fe_{0.55}Ti_{0.45}O_{3-\delta}$ sample microstructure was characterized using a JEM 2010F high-resolution transmission electron microscope (TEM). TEM specimens were prepared by cutting samples into slices, mechanically polishing and finally ion-thinning to electron transparency using a Gatan Precision Ion Polishing System (PIPS).

Dense tubes of $La_{0.2}Sr_{0.8}Fe_{0.8}Cr_{0.2}O_{3-\delta}$ for membrane studies were formed by cold isostatic pressing at 276,000 kPa. The sample was then sintered at 1150 °C for 8 h with heating and cooling rates of 1 °C/min. The two ends were cut and polished to provide parallel surfaces for sealing in the membrane reactor. The final fired dimensions were 6.0 mm o. d., 4.3 mm i.d by 12.0 mm long. A very slight non-concentricity resulted in a wall thickness of 0.85±0.05 mm. The membrane was incorporated into a reactor assembly shown schematically in Fig. 1. Briefly, the membrane was sealed by gold washers to a quartz air tube on top and a quartz disc on bottom. A re-entrant tube allows for positive air flow to the (inner) air side while an outer tube confines an annular down-flow to the syngas side gas. Constant sealing pressure is applied along the membrane axis. Both gas streams (inlet and/or outlet) can be analyzed by on-line gas chromatography or mass spectrometry. A high-gradient, high flux condition was established with synthetic "air" (20% O_2/N_2) on one side and a CO/CO_2 mixture on the other (see Table 1). After achieving steady flux conditions, the oxygen on the air side was switched to $^{18}O_2$ (99%, Isotec) for a fixed time (20%$^{18}O_2$/Ar) while maintaining a constant pO_2 and flow rate. Fig. 1 shows an illustration of the isotope transient experiment. The back exchange of ^{18}O into the air side gas after the isotopic

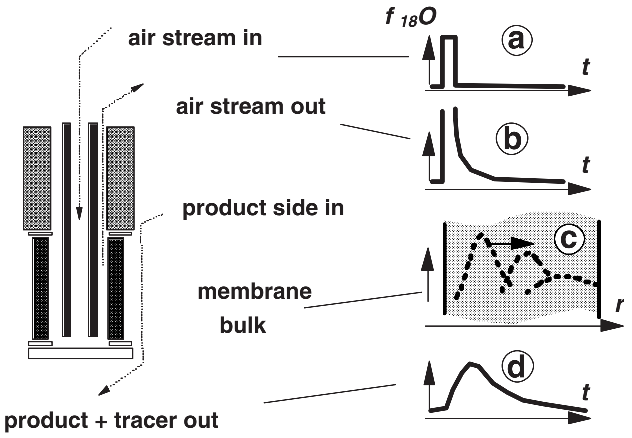

Fig. 1. Membrane reactor and isotope transient experiment diagrams: the left side is a vertical cross-section of the tubular membrane, concentric inner oxygen delivery tube and sealing arrangement. An additional concentric outer tube is not shown. Arrows indicate the gas flows. The right side shows conceptual ^{18}O isotope transient behavior (fraction ^{18}O as a function of time). From the top, the curves show schematically (a) the delivered isotope pulse and (b) the isotope decay transient in the air-side gas arising from back exchange with the solid, (c) the ^{18}O distribution as a function of radius across the membrane wall at a sequence of three times during the transient and (d) ^{18}O in the outer product gas (CO and/or CO_2).